



## Open Research Online

### Citation

Gow, Jason P. D.; Holland, Andrew D.; Pool, Peter J. and Smith, David R. (2012). The effect of protons on the performance of second generation Swept Charge Devices. Nuclear Instruments and Methods in Physics Research Section A: Accelerators, Spectrometers, Detectors and Associated Equipment, 680 pp. 86–89.

### URL

<https://oro.open.ac.uk/33746/>

### License

None Specified

### Policy

This document has been downloaded from Open Research Online, The Open University's repository of research publications. This version is being made available in accordance with Open Research Online policies available from [Open Research Online \(ORO\) Policies](#)

### Versions

If this document is identified as the Author Accepted Manuscript it is the version after peer review but before type setting, copy editing or publisher branding

# The Effect of Protons on the Performance of Second Generation Swept Charge Devices

Jason P. D. Gow<sup>a,\*</sup> Andrew D. Holland<sup>a</sup> Peter J. Pool<sup>b</sup>  
David R. Smith<sup>c</sup>

<sup>a</sup>*e2v centre for electronic imaging, Planetary and Space Sciences Research  
Institute,*

*The Open University, Walton Hall, Milton Keynes MK7 6AA, UK*

<sup>b</sup>*e2v technologies plc, 106 Waterhouse Lane, Chelmsford, Essex, CM1 2QU, UK*

<sup>c</sup>*Centre for Sensors and Instrumentation, School of Engineering and Design,  
Brunel University, Uxbridge, Middlesex, UB8 3PH, UK*

---

## Abstract

The e2v technologies Swept Charge Device (SCD) was developed as a large area detector for X-ray Fluorescence (XRF) analysis, achieving near Fano-limited spectroscopy at -15 °C. The SCD was flown in the XRF instruments on board the European Space Agency's SMART-1 and the Indian Space Research Organisation's Chandrayaan-1 lunar missions. The second generation SCD, proposed for use in the soft X-ray spectrometer on the Chandrayaan-2 lunar orbiter and the soft X-ray imager on China's HXMT mission, was developed, in part, using the findings of the radiation damage studies performed for the Chandrayaan-1 X-ray Spectrometer. This paper discusses the factor of two improvement in radiation tolerance achieved in the second generation SCD, the different SCD sizes produced and their advantages for future XRF instruments, for example through reduced shielding mass or higher operating temperatures.

*Key words:* Swept Charge Device, CCD, proton radiation effects, X-ray fluorescence

---

\* Corresponding author:

*Email address:* j.p.d.gow@open.ac.uk (Jason P. D. Gow).

## 1 Introduction

The surface of the Moon, our closest extraterrestrial neighbour, was first observed and recorded in 1609 by Galileo. Its origin has long been the subject of debate with a number of different theories being put forward. The prevailing theory today is that the Moon formed as a result of the impact of a large body named ‘Theia’, known as the ‘impact trigger’ or ‘giant impact hypotheses’ [1]. In order to understand the formation of the Moon it is essential to characterise the Moon’s surface, which can be achieved through, for example, manned or robotic exploration and orbital X-ray fluorescence (XRF) analysis. Rovers have limited range from their surface landing point and manned missions are costly, whereas space based XRF detector’s can provide elemental abundance information over a large area of the Moon’s surface. One such detector is the e2v technologies plc. Swept Charge Device (SCD). The SCD is a specialist device so does not currently warrant inclusion on the e2v website.

The first SCD was developed as a large area detector for XRF analysis as part of the IMPACT programme [2]. It has now been flown successfully as part of the Development of a Compact Imaging X-ray Spectrometer (D-CIXS) onboard the European Space Agency SMART-1 [3] and the Chandrayaan-1 X-ray Spectrometer (C1XS) onboard the Indian Space Research Organisation (ISRO) Chandrayaan-1 spacecraft [4]. In both cases the energy resolution of the detectors decreased as a result of radiation damage [5,6] arising from the hostile space radiation environment [7]. A number of studies were performed as part of the C1XS radiation damage assessment to investigate the effect of protons on device performance [6,8–11] with the aim of improving instrument performance and recommending modifications to the SCD structure for improved radiation hardness.

This paper will describe the differences between the first and second generation swept charge devices [12], the resulting improvement in radiation hardness and its impact on using the SCD for applications in the space radiation environment.

## 2 The Swept Charge Device

The first SCD, e2v designation CCD54, was developed in 1997 at e2v technologies plc. [2], then EEV ltd., as a possible replacement for the PIN diode detector in spectroscopy applications. The electrode structure is similar to that of a conventional CCD, however it does not provide a pixellated image and is essentially a continuously-clocked linear CCD with a large detection area [6]. The CCD54, a simple schematic of which is illustrated in Figure 1,

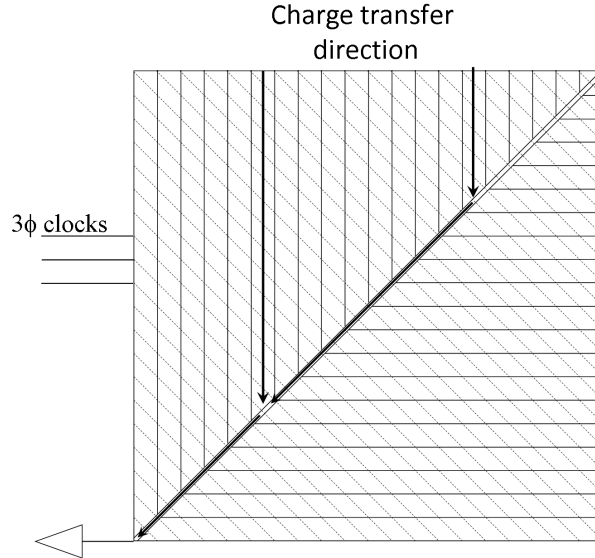


Fig. 1. Schematic of the CCD54, the electrodes are depicted as dashed lines whilst the charge transport channels are indicated using solid lines [6]

has a  $1.07 \text{ cm}^2$  active area covered with 1725 diagonal electrodes depicted by dashed lines, with the column isolation structures ( $25 \mu\text{m}$  pitch) depicted by solid lines, arranged in a herringbone structure. Charge generated in the two triangular charge collection areas is clocked using a three-phase operation towards one of two central read-out channels which are combined prior to the output node. One read-out of the entire detector area creates a linear “image” of 575 “pixels”. They are not true pixels because the SCD has no spatial resolution, however the charge collection, storage and transfer structure is exactly the same as a conventional CCD pixel. A detailed description of SCD operation can be found in [6] and [11].

The column isolation structures of the second generation of SCD are arranged in a perpendicular structure, illustrated in Figure 2, with  $100 \mu\text{m}$  square “pixels”. Due to the increased “pixel” size the probability that charge deposited by an incident X-ray is collected within one “pixel” is increased, reducing the proportion of split events [12]. The particular two-phase “pixel” structure is designed to allow efficient transfer over an unusually large “pixel”, and this structure also ensures that charge is transferred within a narrow channel to minimise charge transfer inefficiency (CTI) for improved radiation hardness. The increased pixel size reduces the number of electrodes within the device and therefore the number of clock cycles required to clear the device, reducing the effect of CTI and reducing the read time. Two-phase clocking simplifies operation, and real and dummy outputs are included to allow, when operated differentially, the suppression of clock-induced pick-up from the video signal. The two central read-out channels in the first generation CCD54 contributed significantly to the observed decrease in energy resolution as a result of radiation induced CTI [11]. The decrease in volume in the central transport channel

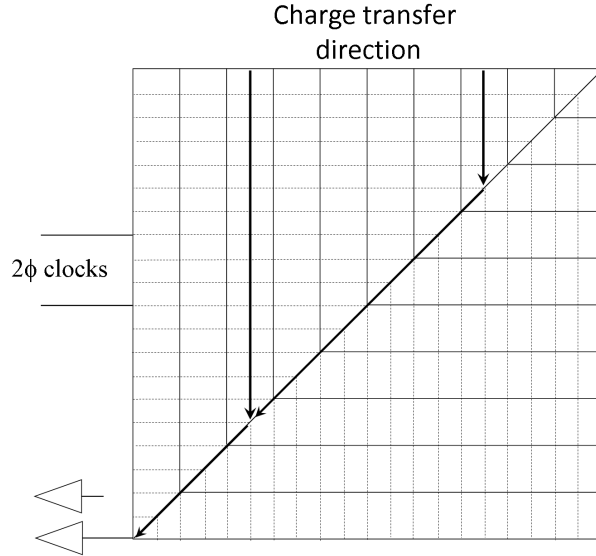


Fig. 2. Schematic of the CCD234, the electrodes are depicted as dashed lines whilst the charge transport channels are indicated using solid lines

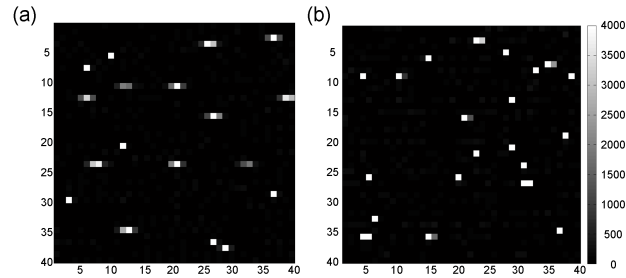


Fig. 3. A  $40 \times 40$  sample section of an image showing Cu-K $\alpha$  and Cu-K $\beta$  X-ray events taken using a CCD54 (a) and a CCD236 (b)

achieved using only one read-out channel, combined with a “pixel” structure which constrains charge during transfer through what is now a “pixel” length of  $141.4 \mu\text{m}$  have been implemented to reduce this effect.

Due to the read-out of the SCD, X-ray events split between “pixels” in parallel channels will be recombined by the transfer structure, whereas charge split across “pixels” which transfer in the same channel will remain split. An example read-out of Cu-K $\alpha$  and Cu-K $\beta$  X-ray events is illustrated in Figure 3(a) for the CCD54 and Figure 3(b) for a second generation SCD (CCD236), clearly demonstrating the improvement in isolated event fraction. The second generation device identified 71% of Cu-K $\alpha$  X-ray events as isolated [13] using an event threshold of twice the standard deviation of the noise peak, compared to an identification of 44% of events in the CCD54 [6].

The second generation of SCD were developed to provide improved radiation hardness, faster readout speed, and increased flexibility in operating temperature. The three variants of the second generation SCD, the two discussed

Table 1

Key parameters for the second generation of swept charge device

Parameter	CCD234	CCD236
Active dimensions (mm)	$10.1 \times 10.1$	$21.1 \times 20.8$
Sensitive area (mm <sup>2</sup> )	110	420
Charge storage capacity	100 ke <sup>-</sup>	100 ke <sup>-</sup>

in this paper are described in Table 1. The smallest area device, CCD235, is suitable for high flux environments where a high readout speed is essential and is capable of achieving Fano limited performance at +10 °C [12], further information on the CCD235 can be found in [12] as the CCD235 formed no part of this study. The CCD234 is comparable in size to the CCD54, and the large active area of the CCD236 makes it suitable for low flux environments and allows increased active area without the requirement for increased drive electronics. The CCD236 is essentially four CCD234 devices in a four leaf clover design, with the central read-out channels combined prior to the read-out node. This clover leaf layout [13] allows this large area device to be read with a minimum number of clock cycles.

The CCD236 is proposed to be used in the ISRO Chandrayaan-2 Large Area Soft X-ray Spectrometer [14] and in the soft X-ray detector on the China National Space Administration Hard X-ray Modulation Telescope (HXMT) spacecraft [15].

### 3 SCD Characterisation and Proton Irradiation

The CCD234 and CCD236 epitaxial devices formed the basis of this study, with each device characterised before and after a proton irradiation. The device under test was held inside the standard e2v centre for electronic imaging test chamber [13], a schematic of which is illustrated in Figure 4. SCD clock and bias potentials were provided by XCAM ltd. CCD drive electronics [16], with event recognition and data analysis performed using custom MatLab software. To provide an insight into device performance in an XRF instrument, data were collected with the device operating between +10 °C and -35 °C, at 120 kHz. Only isolated events were used in the analysis. Further details on the experimental setup and device operation can be found in [13].

The cyclotron at the Kernfysisch Versneller Instituut (KVI) in the Netherlands [17] was used to deliver 50 MeV protons to a displacement damage equivalent of  $3.0 \times 10^8$  10 MeV protons.cm<sup>-2</sup> to a CCD234 and CCD236 device. This fluence was comparable to that used previous CCD54 irradiations [10]. Based on a launch date of October 2009 and the shielding specification of C1XS [4], the fluence of  $3.0 \times 10^8$  10 MeV protons.cm<sup>-2</sup> is equivalent to a third of the

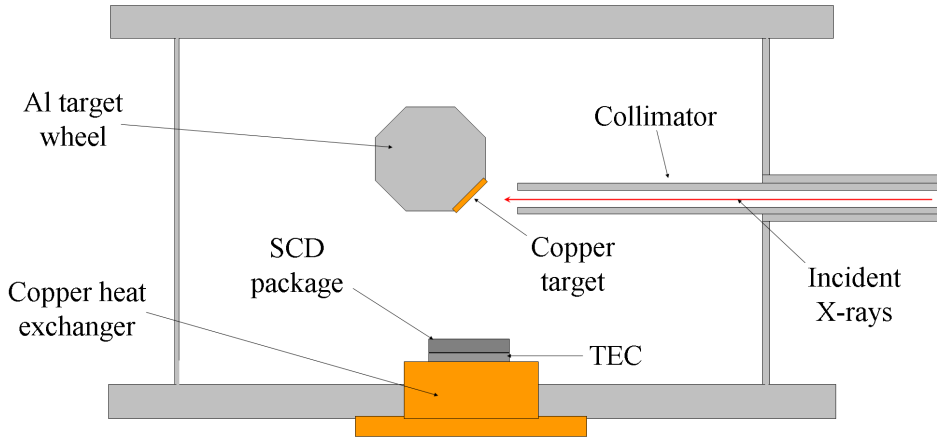


Fig. 4. Schematic of the SCD test facility

total end of life fluence. The predicted fluence was calculated using the ESA SPace ENVironment Information System (SPENVIS) [18].

#### 4 Post Irradiation Analysis

The CCD54 and CCD234 devices demonstrated similar pre and post irradiation levels of dark current, the results are illustrated in Figure 5, as would be expected by devices with comparable active areas. The CCD236 demonstrated a factor of  $\times 4$  higher dark current than the CCD234, as a result of having a detector area  $\times 4$  greater in size. Due to its non-imaging nature, the SCD does not possess regions of prescan or overscan, therefore the dark current was estimated by subtracting the square of the system noise from the total measured noise, where the total noise includes the system and read noise components. It should be noted that the CCD54 was readout at 100 kHz and the CCD234 and CCD236 readout at 120 kHz, therefore to account for the different readout times, i.e. the time during which dark current will be integrated, the values were normalised to 100 kHz to be comparable with the readout rate of the CCD54. Dark current measurements were performed over a small temperature range for the CCD234 and CCD236 pre-irradiation due to time constraints prior to the irradiation date.

The pre-irradiation Cu-K $\alpha$  energy resolution of the CCD54 and CCD234 were found to be comparable, within error, below -2 °C. Post irradiation the energy resolution of the CCD234 as a function of temperature is better than the CCD54, as illustrated in Figure 6. The dark current performance of the CCD234 and CCD54 is similar; therefore the improvement in radiation hardness is as a result of the changes to device structure and operation. The CCD234 provides over a factor of 2 less decreases in energy resolution below -20 °C when compared to the CCD54. The large area of CCD236 results

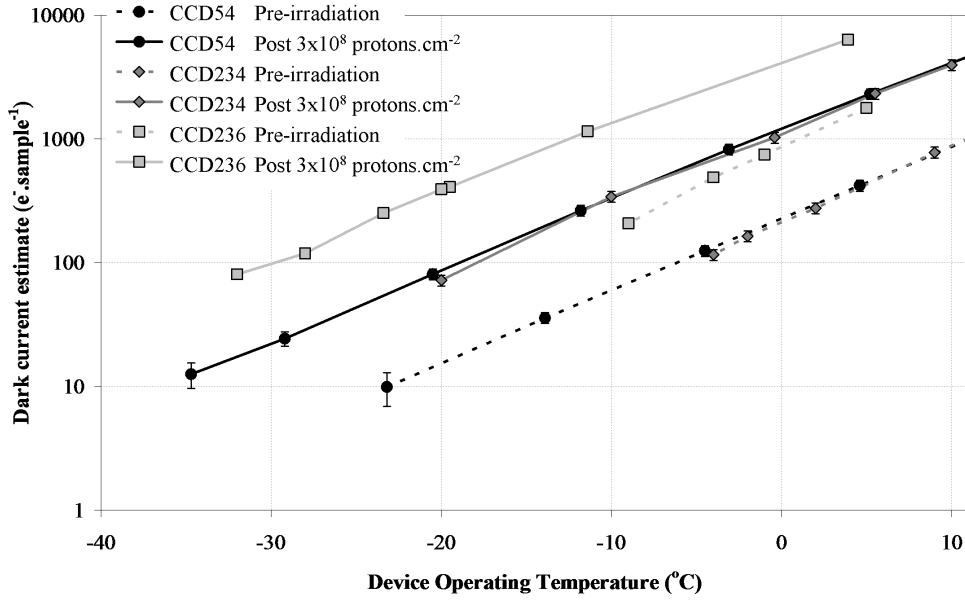


Fig. 5. Estimated dark current as a function of temperature for the CCD54, CCD234, and CCD236 pre and post irradiation

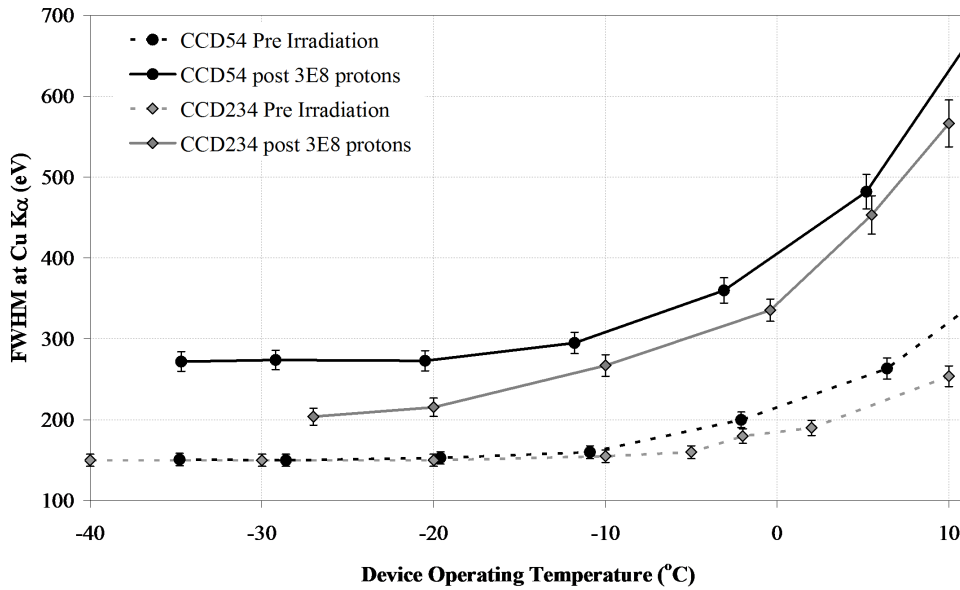


Fig. 6. Energy resolution measured using the Cu-K $\alpha$  X-ray peak as a function of temperature for the CCD54 and CCD234 pre and post irradiation

in higher dark current, however the improvements to minimise radiation induced CTI allow for comparable performance with the smaller CCD54 below  $-26$  °C, illustrated in Figure 7. Below  $-28$  °C the energy resolution measurements made using the CCD236 appear to be better than those made using the CCD54, however the results are within error. Future work will include modifications to the test equipment to allow the CCD236 to be operated at lower temperatures, allowing radiation induced dark current to be to be minimised.

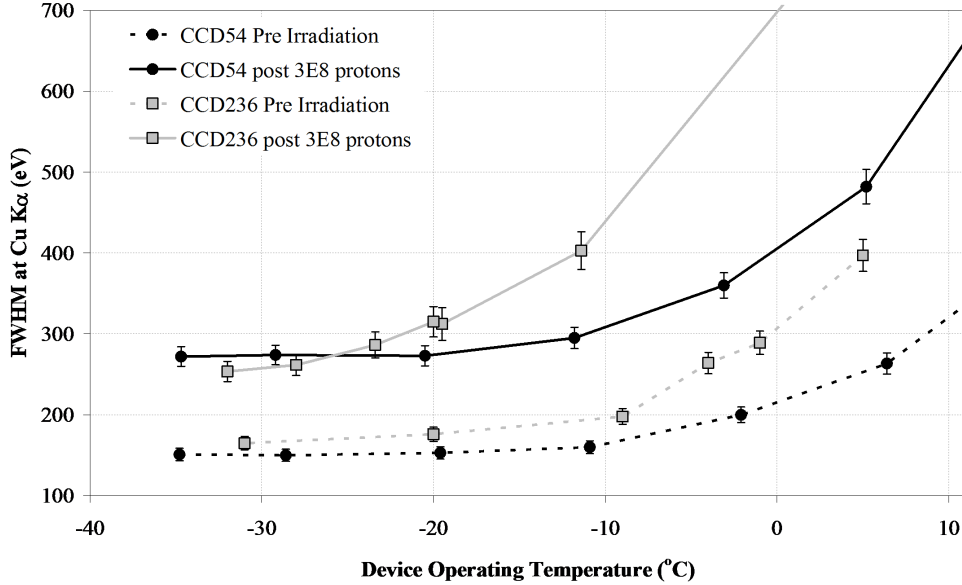


Fig. 7. Energy resolution measured using the Cu-K $\alpha$  X-ray peak as a function of temperature for the CCD54 and CCD236 pre and post irradiation

The C1XS 10 MeV equivalent proton fluence for 2 years at the Moon was estimated, using SPENVIS, to be  $7.5 \times 10^8$  protons.cm $^{-2}$ , assuming the front  $2\pi$  to be shielded by the close proximity to the lunar surface and the rear  $2\pi$  to be shielded with the equivalent of 29 mm of aluminium [6]. Assuming a linear decrease in performance with proton fluence, as demonstrated with the CCD54 [6], to achieve comparable performance to that of a CCD54 based instrument with the same detector area operating at -30 °C an instrument using CCD234 devices would require around 65% less aluminium equivalent shielding while using the CCD236 would require around 25% less. It should also be noted that an instrument using the CCD236 would require less drive electronics than an instrument of comparable detector area using the CCD234, further reducing instrument mass. Further irradiations and a detailed optimisation study are planned for future work in support of the Chandrayaan-2 Large Area Soft X-ray Spectrometer (CLASS) instrument which will use the CCD236 [14].

## 5 Conclusion

Through the improvement in the radiation tolerance of the SCD, in the case of the second generation by around a factor of 2, the performance of future space based XRF instruments can be improved leading to an increase in the quality of data collected. The improvement also allows for other options, for example a reduced quantity of drive electronics, reduced shielding mass, increased detector area and increased operating temperature. The advantage of the SCD over a standard two dimensional CCD is the reduction in read-out

complexity, and the suppression of the surface-generated dark current through the use of ‘intrinsic dither mode’ clocking [8]. The SCD also has the advantage of obtaining good spectra resolution when operated at room temperature, a standard CCD being typically operated below  $-80\text{ }^{\circ}\text{C}$  for X-ray detection.

After receiving a 10 MeV equivalent fluence of  $3\times 10^8\text{ protons.cm}^{-2}$  a C1XS style instrument [4] operated at  $-20\text{ }^{\circ}\text{C}$  using the CCD234 would require around 50% less shielding to achieve comparable performance with an instrument using the CCD54. An instrument utilising the CCD236 would achieve performance comparable to that of the CCD234 operated at around  $-13\text{ }^{\circ}\text{C}$ , if operated at a temperature of around  $-32\text{ }^{\circ}\text{C}$ . Further optimisation of the clocking scheme and evaluation of devices performance following proton irradiation at different levels is required to increase confidence in the shielding recommendations given and further validate predictions of in-flight performance.

## References

- [1] W. K. Hartmann and D. R. Davis, *Icarus*, vol. 24, (1975) 504-515
- [2] A. D. Holland and I. B. Hutchinson, Testing Report for IMPACT ERD2 CCDs, Space Research Centre Leicester University (1998)
- [3] M. Grande, et al., *Planet. Space Sci.*, vol. 51 (2003) 427
- [4] C.J. Howe, et al., *Planet. Space Sci.*, vol. 57 (2009) 735
- [5] M. Grande, et al., *Planet. Space Sci.*, vol. 55, (2007) 494
- [6] J. Gow, Brunel University PhD thesis (2009)
- [7] A. Holmes-Siedle, A. Holland and S. Watts, *IEEE Trans. Nucl. Sci.*, vol. 43 (1989) 2998-3004
- [8] A. D. Holland, et al., *Nucl. Instr. and Meth. A* 521 (2004) 393
- [9] D. R. Smith, J. Gow and A. D. Holland, *Nucl. Instr. and Meth. A* 583 (2007) 270
- [10] D. R. Smith and J. Gow, *Nucl. Instr. and Meth. A* 604 (2009) 177
- [11] J. Gow, et al., *Proc. SPIE* 6686 (2007)
- [12] A. D. Holland and P. Pool, *Proc. SPIE* 7021 (2008)
- [13] J. Gow, A. D. Holland and P. Pool, *Proc. SPIE* 7435 (2009)
- [14] V. Radhakrishna, et al., 42nd Lunar and Planetary Science Conference (2011) 1708
- [15] F. J. Lu, et al., *Proc. of the RIKEN Symposium* (2009) 368

- [16] XCAM Ltd, Scientific CCD Camera Drive System System Operating Manual (2011)
- [17] E. R. van der Graaf, et al, RADECS (2009) 451
- [18] Heynderickx D., et al., J. Proc. AIAA 0371 (2000)